

ОБЪЕДИНЕННЫЙ  
ИНСТИТУТ  
ЯДЕРНЫХ  
ИССЛЕДОВАНИЙ

Дубна

E7-96-82

**Yu. A. Lazarev**

EXTREMES OF NUCLEAR STRUCTURE: DISCOVERY  
OF THE SHELL CLOSURES  $N = 162$  AND  $Z = 108$

Submitted to Proceedings of the XXIV International Workshop on Gross  
Properties of Nuclei and Nuclear Excitations, Hirschegg, Kleinwalsertal,  
Austria, 15—20 January 1996

Макет Т.Е.Попеко

Подписано в печать 29.03.96

Формат 60 × 90/16. Offsetная печать. Уч.-изд. листов 1,22

Тираж 325. Заказ 48996. Цена 1464 р.

Издательский отдел Объединенного института ядерных исследований  
Дубна Московской области

1996



## 1 Introduction

The stability of heavy nuclei is governed by nuclear shell structure whose influence is dramatically amplified near closed proton and neutron shells. Beyond the spherical shells  $Z=82$  and  $N=126$ , the stability of nuclei diminishes rapidly with increasing  $Z$  until the transuranium region, where this trend is altered due to the influence of shell gaps in single-particle level spectra near  $Z=100$  and  $N=152$  that appear here at deformed shapes and provide the unusual stability of  $^{252}\text{Fm}$  against spontaneous fission (SF). Since the mid-1960's, nuclear theory has been predicting with increasing confidence the next spherical shells be located at  $Z=114$  and  $N\approx 178-184$  (see, e.g., reviews [1,2]). More recently, it was realized that this region of spherical superheavy nuclides might be connected by a "peninsula" of stability to the edge of the known heaviest elements. This far-reaching conclusion was based on the predicted existence of the deformed proton and neutron shell closures near  $Z\approx 108$  and  $N\approx 162$  (see, e.g., Refs. [1-4]).

In 1993-1995, we carried out a series of experiments [5-10] designed to provide a direct and decisive test of the theoretical predictions regarding the existence of the new shell closures in the vicinity of  $Z=108$  and  $N=162$ . Prior to our experiments, *no evidence* was available to make a definite conclusion about these predictions. The only exception was the 5-ms nuclide  $^{252}\text{102}$  showing a hint of unexpected stability against SF at  $N=160$  [11].

## 2 Experimental Technique

In our experiments, beams of heavy-ion projectiles were delivered by the JINR U400 cyclotron. The time structure of the pulsed beams was determined by the cyclotron modulating frequency of 150 Hz and a duty factor of  $\approx 40\%$ , which corresponds to a beam cycle of 6.7 ms and a beam pulse duration of  $\approx 2.7$  ms. Rotating targets made of isotopically enriched materials  $^{238}\text{U}$ ,  $^{244}\text{Pu}$ , or  $^{248}\text{Cm}$  were used. A summary of the main bombardments is given in Table I.

**Table I.** Summary of the main bombardments performed in 1993–1995 by employing the Dubna gas-filled recoil separator. Here  $W$  is the average target thickness,  $E$  the bombarding energy in the middle of the target,  $T$  the actual duration of the bombardment (i.e., the pure measurement time),  $D$  the total beam dose, and  $\sigma$  the production cross section (with an estimated accuracy of a factor of  $\sim 3$ ).

Reaction	$W$ mg cm <sup>-2</sup>	$E$ MeV	$T$ h	$D$ 10 <sup>19</sup>	Observed nuclide	$\sigma$ pb
<sup>248</sup> Cm+ <sup>22</sup> Ne	0.24	116	230	1.0	<sup>266</sup> 106, <sup>262</sup> 104	80
		121	131	0.6	<sup>265</sup> 106	260
<sup>244</sup> Pu+ <sup>22</sup> Ne <sup>a)</sup>	0.41	114	122	0.3	<sup>266</sup> 106, <sup>262</sup> 104	60
		120	138	0.2	<sup>261</sup> 104	3500 <sup>b)</sup>
<sup>238</sup> U+ <sup>26</sup> Mg <sup>a)</sup>	0.28	140	146	0.2	<sup>261</sup> 104	2900 <sup>b)</sup>
<sup>238</sup> U+ <sup>34</sup> S	0.54	186	860	1.7	<sup>259</sup> 104	1100 <sup>b)</sup>
<sup>238</sup> U+ <sup>40</sup> Ar <sup>a)</sup>	0.54	214	325	0.6	<sup>267</sup> 108	2.5
<sup>244</sup> Pu+ <sup>34</sup> S <sup>a)</sup>	0.41	190	1375	2.5	<sup>273</sup> 110	0.4 <sup>b)</sup>

<sup>a)</sup> The data from these reactions are still under analysis.

<sup>b)</sup> Preliminary values.

Evaporation residues (EVRs) recoiling out of the targets were separated in flight from beam particles and various transfer-reaction products by the Dubna gas-filled recoil separator [12] shown in Fig. 1. The field  $B$  of the separator's dipole magnet was adjusted to center the quasi-Gaussian distribution of EVRs on the focal-plane detector in the horizontal direction. To solve the nontrivial problem of setting the  $B$  value for a given EVR velocity and  $Z$ , we have performed extensive measurements of average charge states  $\langle q \rangle$  of heavy atoms with  $Z=89$  through  $Z=104$  traversing dilute hydrogen with average velocities  $\langle v/v_0 \rangle$  of 1.0 to 2.5 ( $v_0=2.19 \times 10^6$  ms<sup>-1</sup> is the Bohr velocity). The systematics of the measured  $\langle q \rangle$  values is shown in Fig. 2; it allows interesting atomic physics observations to be made.

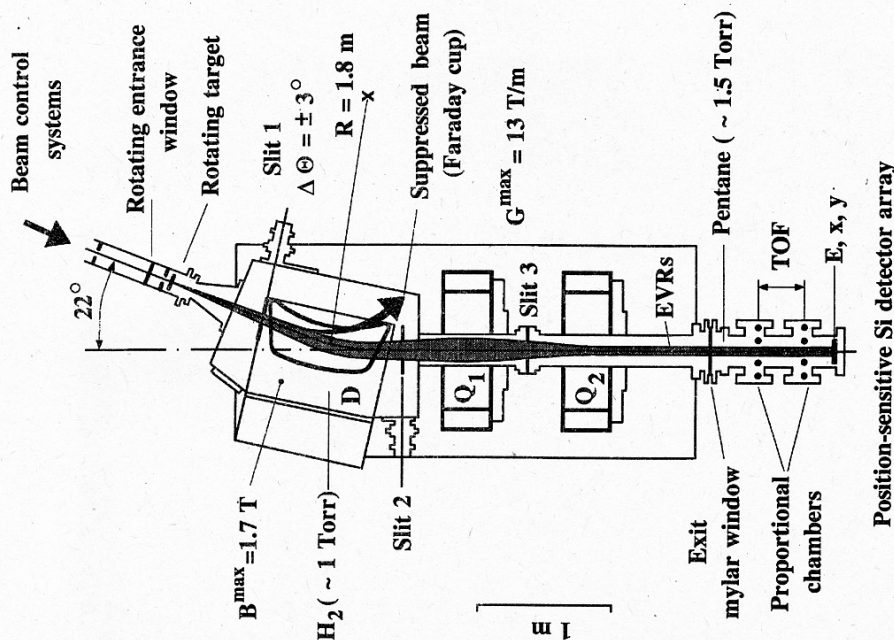


**Fig. 1.** Lay-out of the Dubna gas-filled recoil separator (the dipole magnet D followed by the quadrupole doublet Q<sub>1</sub>Q<sub>2</sub> [12]). The separator is filled with hydrogen at a pressure of about 1 Torr. A 0.5- $\mu$ m "exit" mylar window separates the pentane-filled detection module (see Fig. 3) from the gas media of the separator.

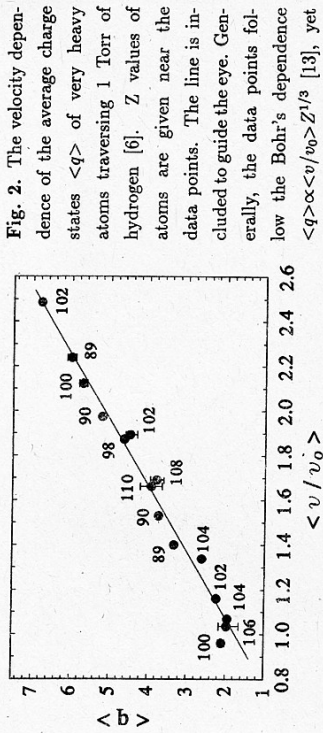


Fig. 2. The velocity dependence of the average charge states  $\langle q \rangle$  of very heavy atoms traversing 1 Torr of hydrogen [6]. Z values of atoms are given near the data points. The line is included to guide the eye. Generally, the data points follow the Bohr's dependence  $\langle q \rangle \propto \langle v/v_0 \rangle^{1/3}$  [13], yet significant deviations from this dependence are seen at low  $\langle v/v_0 \rangle$  values for atoms with  $Z=100$  through 106.

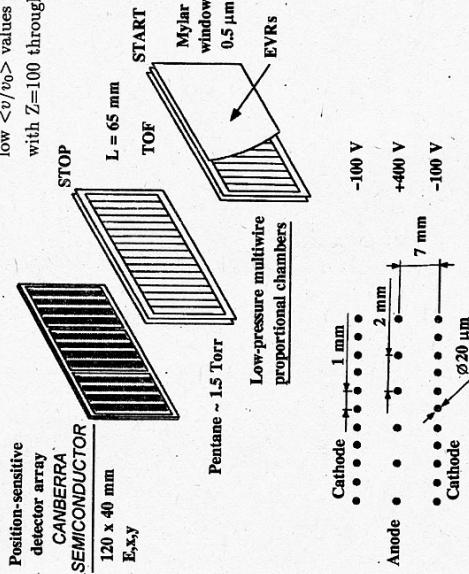
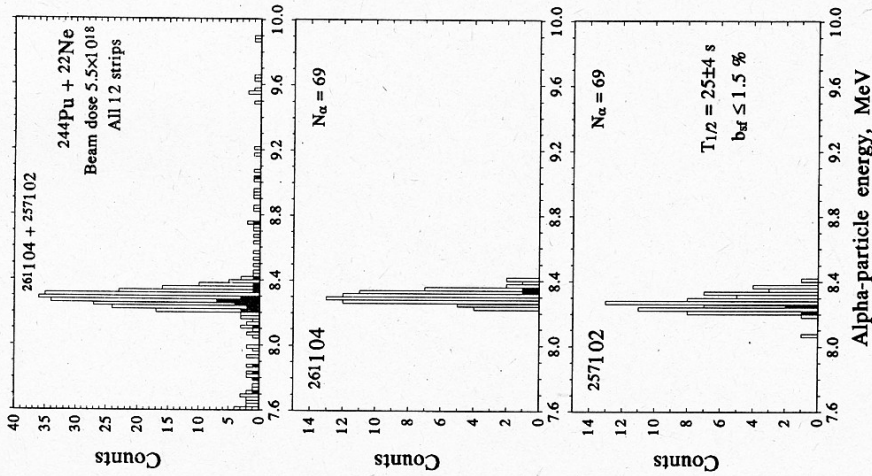


Fig. 3. Detection system of the Dubna gas-filled recoil separator. Two (start and stop)  $140 \times 60 \text{ mm}^2$  multiwire proportional chambers placed in a 1.5-Torr pentane-filled module are used for TOF measurements of EVRS and background particles arriving at the PSD array. The PSD array is composed of three  $40 \times 40 \text{ mm}^2$  passivated boron implanted planar silicon (PIPS) detectors, with each detector having four  $40\text{-mm}$  high  $\times$   $9.7\text{-mm}$  wide strips.

Fig. 4. Energy spectrum of  $\alpha$  particles detected between cyclotron beam pulses in all 12 strips in the 260 h bombardment of  $^{244}\text{Pu}$  with  $5.5 \times 10^{18}$  particles of  $^{22}\text{Ne}$  (upper panel); in the whole  $E_\alpha$  region of 7.6 to 10.0 MeV (actually to 12.0 MeV) the only  $\alpha$  peak is that from  $\alpha$  decays of  $^{261}\text{104}$  and  $^{257}\text{102}$  having similar  $\alpha$ -particle energies. Two lower panels show  $\alpha$ -particle energy spectra of  $^{261}\text{104}$  and  $^{257}\text{102}$ , which were observed from the 69 detected  $\alpha$ - $\alpha$  correlations formed by genetically linked  $\alpha$ -decay events of these two nuclides (see Section 3). Counts shaded in black are those coincident with conversion electrons accompanying the  $\alpha$  decay of  $^{261}\text{104}$  and  $^{257}\text{102}$ , which were detected between cyclotron beam pulses by the stop proportional chamber (see Fig.3). An additional amplifier with highly increased gain was used to process low-amplitude  $\Delta E$  signals from the stop chamber. The relative timing for the coincidences was set to be  $\sim 5 \mu\text{s}$ .





The separated EVRs passed through a time-of-flight (TOF) measurement system composed of two multiwire proportional chambers and were implanted in a  $120 \times 40$  mm<sup>2</sup> position-sensitive detector (PSD) array, see Fig. 3. The PSD array used in our experiments to produce the heaviest isotopes of element 106 is described in Ref. [5]. The 12 strip PSD array used in subsequent experiments was composed of silicon detectors produced by *Camberra Semiconductor NV* (Belgium). We obtained horizontal ( $x$ ) positions for the reaction products from the 12 strips and vertical ( $y$ ) positions from the 40-mm high resistive layer of the detectors. With each detected energy event, we also recorded the strip number, TOF information, the time in  $\mu$ s from the beginning of each beam pulse to either  $\alpha$ /implant or SF events, and the running time in 0.1-ms intervals. The identification of the new nuclides was performed by measuring correlations in energy, time and position to establish genetic links between their implantation in the PSD array and subsequent  $\alpha$  decay followed by  $\alpha$  or SF decays of known descendant nuclides. The potentialities of the gas-filled separator for heavy element research with highly asymmetric fusion-evaporation reactions are demonstrated by our experiments [10] on the production of isotopes of element 104 in the  $^{244}\text{Pu}+^{22}\text{Ne}$  reaction, see Fig. 4.

### 3 Identification and Stability of the New Nuclides $^{262}104$ , $^{265,266}106$ , and $^{267}108$

In the first experiment performed in April 1993 by using the  $^{248}\text{Cm}+^{22}\text{Ne}$  reaction we discovered three new heavy nuclides,  $^{265}106$ ,  $^{266}106$ , and  $^{267}104$  [5]. We observed  $\alpha$  decay with the  $\alpha$ -particle energy  $E_\alpha = 8.63 \pm 0.05$  MeV for  $^{266}106$  and measured a half-life of  $T_{1/2} = 1.2_{-0.3}^{+1.0}$  s for its spontaneously fissioning daughter  $^{262}104$ , thus not confirming a much lower value of  $T_{1/2} = 47$  ms tentatively ascribed to  $^{262}104$  in Ref. [14]. For  $^{265}106$  we measured  $E_\alpha = 8.71$  to 8.91 MeV. From these  $E_\alpha$  energies we estimated partial  $\alpha$ -decay half-lives of 10–30 s for  $^{266}106$  and 2–30 s for  $^{265}106$ . We estimated SF branches of 50% or less for both 106 isotopes. From our data, we set a very conservative  $\alpha$ -branching lower

limit of 15% for  $^{265}106$ . We could not exclude a significant electron-capture (EC) decay branching in the decay of  $^{265}106$ .

After the *unambiguous* identification of the spontaneously fissioning isotope  $^{262}104$  has been made by observing it as the  $\alpha$ -decay daughter of  $^{266}106$  [5], we carried out  $^{244}\text{Pu}+^{22}\text{Ne}$  experiments [10] to probe the  $\alpha$ -decay branch of this key even-even nuclide. We were searching for time and position correlations of  $\alpha$  decays in the  $E_\alpha$  range expected for  $^{262}104$  to subsequent SF events from its spontaneously fissioning daughter  $^{268}102$ . The observation of the  $\alpha$  decay of  $^{262}104$  would give important information for improving predictions of mass excesses and shell corrections for the  $\alpha$ -decay chain with  $N-Z=54$ , involving  $^{266}106$  and the yet undiscovered doubly magic  $N=162$  nuclide  $^{270}108$ . This would also allow the unequivocal identification and the half-life measurement of  $^{268}102$ , which so far is believed to be a short-lived spontaneously fissioning nuclide with  $T_{1/2} = 1.2 \pm 0.2$  ms [15,16].

In the  $^{244}\text{Pu}+^{22}\text{Ne}$  bombardments [10] we detected 69  $\alpha$ - $\alpha$  correlations linking  $\alpha$  decays of  $^{261}104$  and  $^{267}102$ . The half-lives of these two nuclides are known to be similar ( $65 \pm 10$  s and  $25 \pm 2$  s, respectively), while the  $\alpha$  energies of  $^{267}102$  overlap those of  $^{261}104$  [15]. For the first time we were able to observe clearly, for each individual  $\alpha$ -decay event of  $^{261}104$ , a subsequent time- and position-correlated  $\alpha$ -decay event of its genetically related daughter  $^{267}102$ . Let us note here that the nuclides  $^{261}104$  and  $^{267}102$  are the last short-lived descendants in the  $\alpha$  decay series starting from  $^{273}110$  (see Section 4). As shown in the lower panels in Fig. 4, we observed  $\alpha$ -particle energies  $E_\alpha = 8.22$  to 8.41 MeV for  $^{261}104$  and 8.07 (weak), 8.19 to 8.40 MeV for  $^{267}102$ ; conversion electrons coincident with some of these  $\alpha$  decays were detected. The half-life of  $^{267}102$  was measured to be  $25 \pm 4$  s. No correlations were found between  $\alpha$  decays with  $E_\alpha \geq 7.6$  MeV and subsequent SF events within the time window of 10  $\mu$ s to 10 min, from which we calculated the 68% confidence level upper limit of 1.5% for the SF branch of  $^{267}102$  and a preliminary upper limit of 3% for the  $\alpha$ -decay branch of  $^{262}104$ . Both the low  $\alpha$  branching and the predominance of

the SF in the decay of  $^{262}104$  (and all other even-even  $Z=104$  nuclides) is a very definite prediction of the theory [2-4,17]. The most recent theoretical values [17] of the partial half-lives for the  $\alpha$  and SF decay of  $^{262}104$  are 180 s and 0.21 s, respectively; the  $Q_\alpha$  value was predicted to be 8.26 MeV for  $^{262}104$  [17].

The ground-state decay properties that we established for  $^{266}106$  and  $^{262}104$  reveal a large enhancement in their stability as compared to that of nuclides with lower  $Z$  or  $N$  values. For example, the transition from  $^{262}102$  to  $^{266}106$  at  $N=160$  or from  $^{262}104$  to  $^{262}104$  at  $N=158$ , an addition of four protons, increases the stability against SF by a factor of  $\approx 3 \times 10^3$  (see Fig.5). It was observed for the first time that an increase in  $Z$  at a given  $N$  causes an elevation in the SF half-lives of even-even nuclides. The only explanation for this fact can be the approach to a nearby proton shell closure. Similarly, in going from  $^{260}106$  to  $^{266}106$ , the stability increases by a factor of  $\approx 3 \times 10^3$  for SF decay and  $\sim 3 \times 10^3$  for  $\alpha$  decay. Thus, the ground-state decay properties of  $^{262}104$  and  $^{266}106$  provide a strong indication of the existence of deformed shell closures near  $N=162$  and  $Z=108$  (see Fig.6). On the other hand, our data plotted in Fig.3 show that the SF stability at  $Z=106$  and  $N=160$  is *not* reduced by the destabilizing effect of the new fission valley which was predicted by theory to develop close to the fragment magic numbers  $N=2 \times 82$  and  $Z=2 \times 50$ , to extend up to  $Z=110$ , and to lead, with a low collective inertia, to very compact scission shapes and very short SF half-lives in the sub-*ms* range [1]. The discovery of significantly increased nuclear stability near  $N=162$  and  $Z=108$  offered new opportunities for extending the chart of the nuclides at its upper edge. Moreover, this discovery paved the way for detailed studies of chemical properties of the element 106 and nearby elements, including chemistry studies with aqueous solutions. In 1995, first chemical separations of element 106 were performed [21], based on the production of the isotopes  $^{265}106$  and  $^{266}106$  in the  $^{248}\text{Cm} + ^{22}\text{Ne}$  reaction.

In March-April 1994 we carried out experiments designed to explore further the nuclear stability near  $N=162$  and  $Z=108$  by producing new heavy isotopes of element 108 in the

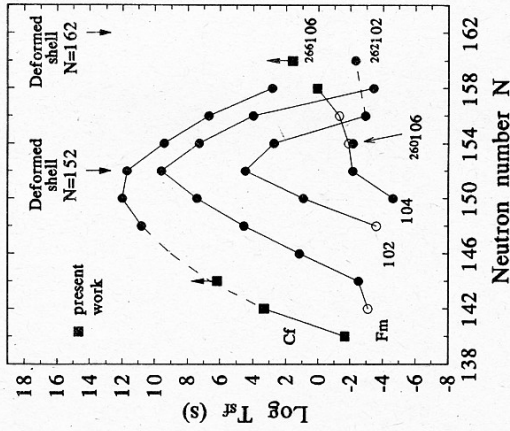


Fig. 5. Partial SF half-lives measured for even-even nuclei with  $Z \geq 98$ . Squares show the data for  $^{262}104$  and  $^{266}106$  from Ref. [5], as well as recent data for the lightest Cf isotopes from Ref. [18]. For origins of other data points, see Refs. [11,15,18-20]. Open data circles are used to mark questionable assignments or/and tentative  $T_{1/2}$  values.

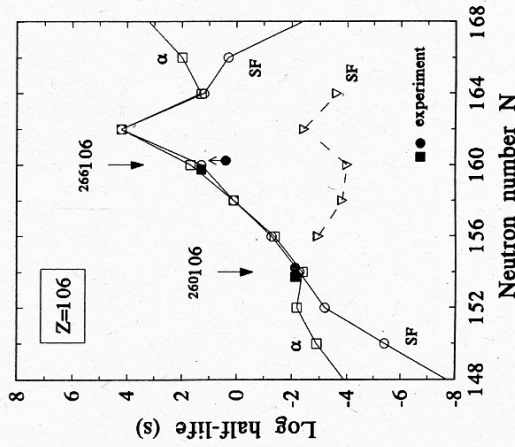


Fig. 6. Predicted partial half-lives [3, 4] for SF and  $\alpha$  decay of the even-even 106 isotopes shown by the lines connecting open circles and squares, respectively. The dashed line connecting the triangular points shows SF half-life predictions from Ref. [1]. The experimental values for  $^{260}106$  [15] and the results for  $^{266}106$  from our work [5] are shown by closed symbols.



complete fusion reaction  $^{238}\text{U}+^{34}\text{S}$ . Another goal of these experiments was to probe cross section values for the actinide-target-based fusion-evaporation reactions leading to the  $Z=108$  nuclides. In a 36-day bombardment we identified the  $\alpha$ -decaying  $N=159$  isotope  $^{267}\text{108}$  with a half-life of  $19^{+29}_{-10}$  ms and  $E_\alpha=9.74$  to  $9.87$  MeV [6]. An important result of this work is the measurement of the 2.5 pb cross section for the  $^{238}\text{U}(^{34}\text{S},5n)$  reaction, which is  $10^5$  times lower than that of the reaction  $^{238}\text{U}(^{22}\text{Ne},5n)$ . This dramatic cross section decrease (see Fig.7) reveals a fusion limitation mechanism *different* from that associated with the overcritical Coulomb-to-nuclear force ratio, in the entrance reaction channel. As an intermediate case, Fig.7 includes the cross section value for the reaction  $^{238}\text{U}(^{26}\text{Mg},5n)$  that we measured in a separate experiment by detecting  $\alpha$ - $\alpha$  correlations linking  $\alpha$  decays of the known nuclides  $^{259}\text{104}$  and  $^{255}\text{102}$ .

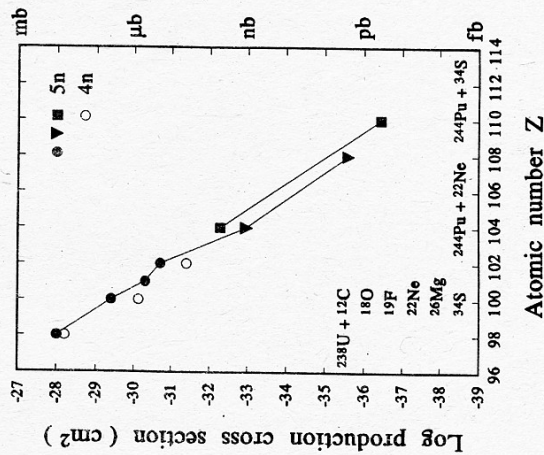


Fig. 7. Measured cross sections for the 4n and 5n evaporation channels of the complete fusion reactions between  $^{238}\text{U}$  and projectiles  $^{12}\text{C}$  through  $^{34}\text{S}$ . The measured cross section for the 5n evaporation channel of the  $^{244}\text{Pu}+^{34}\text{S}$  reaction is shown for comparison. The data points for  $^{26}\text{Mg}$ - and  $^{34}\text{S}$ -induced reactions shown by triangles represent experimental results of the present work. Other data are taken from Refs. [22,23].

#### 4 Identification and Alpha Decay of $^{273}\text{110}$

In our 106 experiment, we found strong evidence for the shell closures near  $N=162$  and  $Z=108$  by exploring the nuclear stability pattern in the region just below these magic nucleon numbers predicted by theory. Another direct test of the theory could be the observation of a decrease in stability for nuclides with  $Z, N$  beyond the predicted magic numbers. This would allow the exact  $Z, N$  localization of the new shell closures. In particular, the determination of whether the neutron closure is at  $N=162$  or at a higher  $N$  value can be made by measuring  $\alpha$ -decay properties of a nuclide with  $N=163$  or  $164$ . As known from  $\alpha$ -decay studies of Po-Th nuclides around the  $N=126$  shell, the  $\alpha$ -decay energy,  $Q_\alpha$ , becomes considerably larger if the shell is crossed and breaks the trend of the  $Q_\alpha$  values decreasing with increasing  $N$  for isotopes of a given  $Z$ . From  $^{209}\text{Po}$  ( $N=125$ ) to  $^{211}\text{Po}$  ( $N=127$ ) the  $Q_\alpha$  value increases by 2.6 MeV and the half-life decreases by  $6 \times 10^9$  times, reflecting the outstanding strength of the  $N=126$  shell.

The choice of feasible target-projectile systems to produce a neutron-rich nuclide with  $N>162$  is strongly limited. "Cold fusion" reactions with  $^{208}\text{Pb}$  or  $^{209}\text{Bi}$  targets allow this to be achieved only at  $Z=112$ . With actinide-target-based fusion-evaporation reactions, the  $N>162$  region is achievable at  $Z=110$ .

During the period from September 10 to December 30, 1994, we carried out experiments at the Dubna U400 cyclotron to produce neutron-rich  $Z=110$  nuclides by the  $^{244}\text{Pu}+^{34}\text{S}$  reaction at the bombarding energy  $E(^{34}\text{S})=190$  MeV, some 6 MeV above the Bass fusion barrier [24], resulting in an excitation energy for the compound nucleus  $^{278}\text{110}$  of  $\approx 50$  MeV. This bombarding energy is expected to provide the maximum yield of  $^{273}\text{110}$ , the 5n evaporation product, although the 4n and 6n channels leading to  $^{274}\text{110}$  and  $^{272}\text{110}$  are also open. During part of the above time period we used the  $^{238}\text{U}+^{40}\text{Ar}$  reaction at  $E(^{40}\text{Ar})=214$  MeV that leads to the same compound system  $^{278}\text{110}$  with the same excitation energy.

We conducted an extensive off-line search of the raw  $^{244}\text{Pu}+^{248}\text{S}$  data for event sequences which fit the expected pattern of implantation in the PSD array and subsequent decay of  $^{273}\text{110}$  and its descendants. As a result, two prominent event sequences were observed (see Table II and Ref. [7]). The first sequence shown in Table II fit best the expected pattern of implantation in the PSD array and subsequent  $\alpha$  decay of the new nuclide  $^{273}\text{110}$  and was produced after 43 days of actual bombardment. This event sequence occurred in the center of the PSD array (5 mm off the vertical-middle of strip 7), where a 6.39-MeV EVR implantation event detected in coincidence with a characteristic TOF signal was followed in 394  $\mu\text{s}$  by an  $\alpha$ -decay event with  $E_{\alpha 1}=11.35$  MeV; then, following this by 158 s, an out-of-beam  $\alpha$ -decay event with  $E_{\alpha 2}=8.63$  MeV was detected, followed 384 s later by a third  $\alpha$ -decay event with  $E_{\alpha 3}=8.22$  MeV. The  $y$ -position signals registered for each member of the sequence revealed a close correlation of the four events on strip 7. On the whole, the correlated EVR- $\alpha$ - $\alpha$  sequence is documented by 14 measured parameters; the main parameters are summarized in Table II.

As shown in Table II, we interpret this correlated event sequence as the  $\alpha$  decay of the new nuclide  $^{273}\text{110}$  followed by two detected  $\alpha$  decays of its descendants,  $^{265}\text{106}$  and  $^{257}\text{102}$ . On the basis of our data we calculate straightforwardly and conservatively that the expected number of random 4-fold correlations of the above type is  $6 \times 10^{-3}$  for the whole PSD array and the entire measurement time  $T=1375$  h.

The three-member event sequence in Table II with  $E_{\alpha 1}=11.72$  MeV also shows the  $^{273}\text{110}$  implantation/decay pattern. The observation of the out-of-beam 8.86-MeV  $\alpha$  event 43 s after the occurrence of the  $\alpha 1$  event lends a great deal of significance to this chain, but there are a number of less perfect features as well. It occurred in strip 1, where the background is some three times higher as compared to the center of the PSD array; the measured EVR energy of 3.81 MeV was at the lower edge of the expected  $\pm 2\sigma$  range of  $Z=110$  EVR energies, and the measured  $\Delta\text{pos}$  values were close to their higher limits. The  $E_{\alpha 1}$  of 11.72 MeV gives a  $Q_{\alpha 1}$  value for this transition of 11.90 MeV, some 0.7 MeV

Table II. The measured parameters of the correlated  $^{273}\text{110}$  event sequences observed in the  $^{244}\text{Pu}+^{248}\text{S}$  reaction.

Particle	Particle energy (MeV)	Strip no.	$\Delta t^d$	$\Delta\text{pos}^e$ (mm)	Assignment	$N_b^f$
EVR <sup>a)</sup>	6.39	7		+1.1	$^{273}\text{110}$	
$\alpha$	11.35	7	394 $\mu\text{s}$		$^{273}\text{110}$	
$\alpha^b$ )	8.63	7	158 s	-0.5	$^{265}\text{106}$	
$\alpha$	8.22	7	384 s	-0.4	$^{257}\text{102}$	0.006
EVR <sup>c)</sup>	3.81	1		+1.4	$^{273}\text{110}$	
$\alpha$	11.72	1	13.2 ms		$^{273}\text{110}$	
$\alpha^b$ )	8.86	1	43 s	-1.0	$^{265}\text{106}$	0.064

<sup>a)</sup>This sequence was detected at 4:49 a.m. on 10 December 1994 after 1041 h of actual bombardment at a beam dose of  $1.9 \times 10^{19}$  particles of  $^{34}\text{S}$ .

<sup>b)</sup>Event occurred between cyclotron beam pulses.

<sup>c)</sup>This sequence was detected at 5:35 a.m. on 14 September 1994 after 56 h of actual bombardment at a beam dose of  $1.1 \times 10^{18}$  particles of  $^{34}\text{S}$ .

<sup>d)</sup>The indicated  $\Delta t$  values are time distances to the preceding event of a given correlation chain.

<sup>e)</sup>The  $y$ -position deviations are given with respect to the  $\alpha 1$  event from  $^{273}\text{110}$ .

<sup>f)</sup>The  $N_b$  values are calculated for the whole PSD array and the entire measurement time of 1375 hours.

higher than is expected from theoretical predictions [2]. This  $Q_{\alpha 1}$  corresponds to an unhindered  $T_{1/2}$  value of 1.5  $\mu\text{s}$  [2], which requires a hindrance factor of  $\sim 6000$  to achieve a  $T_{1/2}$  of 9 ms, as the value of  $\Delta t$ , indicates; such a transition would likely have a low abundance. We should expect the odd-A nuclide  $^{273}\text{110}$  with  $N=N_{\text{magic}}+1$  to have a broad and complex  $\alpha$  spectrum, as it is the case, e.g., for the five known even-Z  $\alpha$  emitters with  $N=153$ ,  $^{251}\text{Cf}$  through  $^{259}\text{106}$  [15]. Different versions of macroscopic-microscopic calculations [1,2,12] definitely predict a striking bunching of single-particle levels with spins and parities  $J\pi$  of  $1^+$ ,  $3^+$ ,  $5^+$ ,  $7^+$ ,  $9^+$  and  $11^-$  of the  $N=157$ , 159, and 161 nuclei, as well as a large,  $\approx 1$ -MeV gap up to the next, clearly isolated  $N=163$  level with  $J\pi=13^-$ , which should result in a large hindrance factor for the  $\alpha$  decay of  $^{273}\text{110}$ , since no  $13^-/2^-$  level can be seen below  $N=163$ .

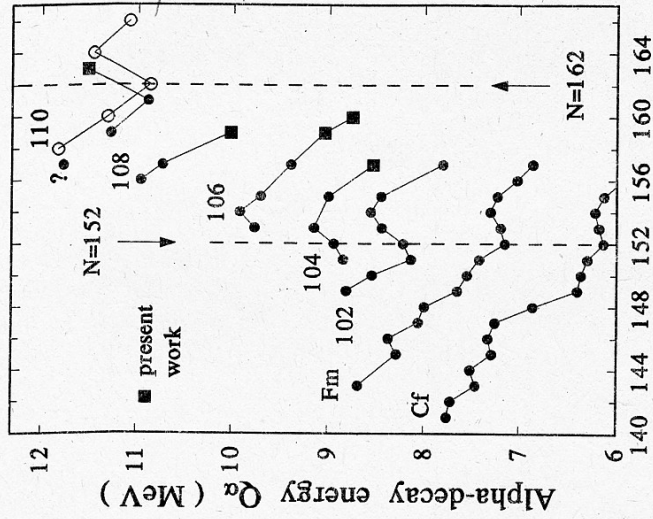


Thus, our detailed analysis of the  $^{244}\text{Pu} + ^{34}\text{S}$  data [7] confirms the uniqueness and the high statistical significance of the 11.35-MeV event sequence belonging to  $^{273}110$ , which was first reported in Refs. [8,9]. The complete analysis reveals other event sequences which deserve further consideration, including that with  $E_{\alpha 1} = 11.72$  MeV, but their significance is lower than the 11.35-MeV chain, and the following discussion will be based on that sequence.

The  $\approx 0.4$ -ms interval between implantation and  $\alpha$  decay of the  $^{273}110$  EVR results in a maximum likelihood  $T_{1/2}$  value of  $0.3^{+1.3}_{-0.2}$  ms (68% confidence interval). Based on one detected chain, the production cross section of  $^{273}110$  at  $E(^{34}\text{S}) = 190$  MeV is roughly 0.4 pb, close to expectations when extrapolated from the 2.5 pb cross section measured for the  $^{238}\text{U}(^{34}\text{S}, 5n)$  reaction [6] (see Fig.7). The cross section estimate for  $^{273}110$  could be higher if we assume an EC branching in the decay of  $^{261}104$ ,  $^{265}106$ , or  $^{269}108$ .

The  $\alpha$ -particle energy  $E_{\alpha} = 11.35$  MeV measured for  $^{273}110$  gives a  $Q_{\alpha}$  of 11.52 MeV when corrected for recoil energy of the daughter nucleus. Such a high  $Q_{\alpha}$  value for the  $Z=110$  nuclide with  $N=163$  provides direct and convincing evidence that a neutron shell closure indeed exists and is located at  $N=162$  and not at a higher value of  $N$ . The  $Q_{\alpha}$  value for  $^{273}110$  would have been about 1 MeV lower if the shell closure had occurred at  $N > 162$ . We illustrate this in Fig. 8 with a plot of  $Q_{\alpha}$  vs  $N$  for isotopes of even- $Z$  elements Cf through 110, including  $Q_{\alpha} \approx 11.3$  and  $\approx 10.9$  MeV for the isotopes  $^{269}110$  and  $^{271}110$  that were identified in  $^{208}\text{Pb} + ^{62,64}\text{Ni}$  experiments conducted at GSI/Darmstadt [26] in the same time period as the present experiment; we also show the point  $Q_{\alpha} \sim 11.8$  MeV from a report [27] on the possible production of  $^{267}110$  in  $^{209}\text{Bi} + ^{60}\text{Co}$  bombardments at LBL/Berkeley. The measured  $E_{\alpha}$  energies for  $Z=110$  were assumed to correspond to the ground-state to ground-state transition. Although the odd- $A$   $Z=110$  nuclides are not expected to decay to the ground state, they would have to decay to daughter energy levels unrealistically different to alter the  $Q_{\alpha}$  vs  $N$  pattern in Fig. 8.

In Fig. 8 one can clearly see the reversal in  $Q_{\alpha}$  vs  $N$  behaviour for  $^{273}110$  as compared



Neutron number  $N$

Fig. 8. Alpha-decay energy  $Q_{\alpha}$  vs neutron number  $N$  for isotopes of even- $Z$  elements Cf through 110 [5-10,15,26,27]. Squares show data from Refs. [5-10], as well as  $Q_{\alpha}$  for  $^{273}110$  from this work. Open circles show theoretical  $Q_{\alpha}$  values [2] for even-even  $Z=110$  isotopes. The neutron numbers  $N_{shell}=152$  and  $N_{shell}=162$  are delineated to emphasize the behaviour of  $Q_{\alpha}$  with  $N$  in the region of shell closures.

with the trend for the lighter  $Z=110$  isotopes. This observation is in good agreement with the recent theoretical  $Q_{\alpha}$  predictions [2] shown in Fig.8. A more detailed comparison of the measured decay properties of  $^{273}110$  with theoretical predictions [1-4,25] is presented in Table III. The 0.6-MeV increase in  $Q_{\alpha}$  between  $N=161$  and  $N=163$  reflects the strength of the shell closure at  $N=162$  and can be contrasted with a  $Q_{\alpha}$  increase of 0.1-0.3 MeV

**Table III.** Comparison of the measured decay properties of  $^{273}110$  with theoretical predictions [1-4,25].

THEORY PREDICTS	EXPERIMENT SAYS
A neutron-deformed shell exists and is at N=162.	<b>Yes</b> , it exists indeed and is at N=162, not at a higher N value.
There should be a clear reversal in $Q_\alpha$ vs N after crossing N=162, not only a flattening like at N=152 <sup>a)</sup> .	<b>Yes</b> , the $Q_\alpha$ reversal for $^{273}110$ is observed.
The N=162 shell should be stronger than the N=152 shell <sup>a)</sup> .	<b>Yes</b> , the N=162 shell is stronger indeed.
Quantitatively, the increment in $Q_\alpha$ between N=162 and N=164 for Z=110 is 0.6 MeV <sup>a)</sup> .	<b>Yes</b> , the $Q_\alpha$ increment between N=161 and N=163 for Z=110 is 0.55 MeV at least. The N=162 shell appears stronger than predicted. But the theory underestimates the strength of the N=152 shell as well.
A high-spin ( $\frac{13}{2}$ ) ground-state for $^{273}110$ , resulting in a large HF for its $\alpha$ decay.	<b>Yes</b> , with $E_\alpha=11.35$ MeV and $T_{1/2}=0.3^{+1.3}_{-0.2}$ ms, the HF is $30^{+130}$ . This is a strongly hindered rather than favoured $\alpha$ decay of the even-odd nuclide $^{273}110$ .

<sup>a)</sup>These predictions have been made in Refs. [2-4].

between N=151 and N=153 in the region of Fm to Z=104, or, alternatively, with that of 1.8-2.6 MeV between N=125 and N=127 in the Po-Th region. The N=162 shell closure appears much weaker than the spherical shell N=126, but seems at least comparable in strength to the deformed shell N=152.

## 5 Conclusions

Table IV summarizes decay properties of the new nuclides discovered in the present series of experiments. We note that these nuclides represent the heaviest isotopes of elements 104, 106, 108, and 110 produced up to now.

**Table IV.** Decay properties of the new heavy nuclides discovered in the present series of experiments.

Nuclide	Principal decay mode	Alpha-particle energy, MeV	Half-life	Ref.
$^{273}110$	$\alpha$	11.35	$0.3^{+1.3}_{-0.2}$ ms	[7,8,9]
$^{267}108$	$\alpha$	9.74 to 9.87	$19^{+29}_{-10}$ ms	[6]
$^{266}106$	$\alpha$	$8.63 \pm 0.05$	10-30 s	[5]
$^{265}106$	$\alpha$	8.63 to 8.91	2-30 s	[5,7]
$^{262}104$	SF		$1.2^{+1.0}_{-0.3}$ s	[5]
$^{238}\text{Cf}$	SF		$21 \pm 2$ ms	[18]

The production and positive identification of the nuclide  $^{273}110$  signifies the observation of the element 110. The principal result of our 110 work is the direct experimental evidence for a strong shell closure at N=162 as determined by the measured  $\alpha$ -decay properties of  $^{273}110$ , the only N=163 nuclide known up to now. Providing a decisive test of and a new credit for the current nuclear theory, this result offers predicted spherical shells at Z=114 and N=178-184 to be a major challenge for future experimental explorations.

I wish to thank F.Sh. Abdullin, Yu.V. Lobanov, A.N. Polyakov, E.A. Shchukina, and V.K. Utyonkov for their essential help in preparing this manuscript. The studies described in the present paper were supported by Grants RFN000 and RFN300 from the International Science Foundation and the Government of the Russian Federation. The  $^{244}\text{Pu}$  target material and a part of the  $^{248}\text{Cm}$  material were provided for the present experiments by the U.S. Department of Energy through the Oak Ridge National Laboratory. These studies were performed in the framework of the Russian Federation/US Joint Coordinating Committee for Research on Fundamental Properties of Matter.



## References

- [1] P. Möller and J.R. Nix, *J. Phys. G* **20**, 1681 (1994).
- [2] R. Smolańczuk and A. Sobiczewski, in *Low Energy Nuclear Dynamics* (World Scientific, Singapore, 1995) p.313.
- [3] Z. Patyk and A. Sobiczewski, *Nucl. Phys.* **A533**, 132 (1991).
- [4] R. Smolańczuk, J. Skalski, and A. Sobiczewski, *Phys. Rev. C* **52**, 1871 (1995).
- [5] Yu.A. Lazarev, Yu.V. Lobanov, Yu.Ts. Oganessian, V.K. Utyonkov, F.Sh. Abdullin, G.V. Buklanov, B.N. Gikal, S. Iliev, A.N. Mezentsev, A.N. Polyakov, I.M. Sedych, I.V. Shirokovsky, V.G. Subbotin, A.M. Sukhov, Yu.S. Tsyganov, V.E. Zhuchko, R.W. Loughheed, K.J. Moody, J.F. Wild, E.K. Hulet, and J.H. McQuaid, *Phys. Rev. Lett.* **73**, 624 (1994).
- [6] Yu.A. Lazarev, Yu.V. Lobanov, Yu.Ts. Oganessian, Yu.S. Tsyganov, V.K. Utyonkov, F.Sh. Abdullin, S. Iliev, A.N. Polyakov, J. Rigol, I.V. Shirokovsky, V.G. Subbotin, A.M. Sukhov, G.V. Buklanov, B.N. Gikal, V.B. Kutner, A.N. Mezentsev, I.M. Sedych, D.V. Vakatov, R.W. Loughheed, J.F. Wild, K.J. Moody, and E.K. Hulet, *Phys. Rev. Lett.* **75**, 1903 (1995).
- [7] Yu.A. Lazarev, Yu.V. Lobanov, Yu.Ts. Oganessian, V.K. Utyonkov, F.Sh. Abdullin, A.N. Polyakov, J. Rigol, I.V. Shirokovsky, Yu.S. Tsyganov, S. Iliev, V.G. Subbotin, A.M. Sukhov, G.V. Buklanov, B.N. Gikal, V.B. Kutner, A.N. Mezentsev, K. Subotic, J.F. Wild, R.W. Loughheed, and K.J. Moody, *JINR Preprint No. E7-95-552*, Dubna, 1995; submitted to *Phys. Rev. C*.
- [8] Yu.A. Lazarev, Yu.V. Lobanov, Yu.Ts. Oganessian, V.K. Utyonkov, F.Sh. Abdullin, A.N. Polyakov, J. Rigol, I.V. Shirokovsky, Yu.S. Tsyganov, S. Iliev, V.G. Subbotin, A.M. Sukhov, G.V. Buklanov, B.N. Gikal, V.B. Kutner, A.N. Mezentsev, I.M. Sedych, K. Subotic, R.W. Loughheed, J.F. Wild, K.J. Moody, and E.K. Hulet, in *Heavy Ion Physics, Scientific Report 1993-1994* (JINR Report No. E7-95-227, Dubna, 1995) p.29.
- [9] Yu.A. Lazarev, in *Low Energy Nuclear Dynamics* (World Scientific, Singapore, 1995) p.293.
- [10] Yu.A. Lazarev, Yu.V. Lobanov, Yu.Ts. Oganessian, V.K. Utyonkov, F.Sh. Abdullin, A.N. Polyakov, J. Rigol, I.V. Shirokovsky, Yu.S. Tsyganov, S. Iliev, V.G. Subbotin, A.M. Sukhov, G.V. Buklanov, K. Subotic, K.J. Moody, N.J. Stoyer, J.F. Wild, and R.W. Loughheed, to be submitted to *Phys. Rev. C*.
- [11] R.W. Loughheed, E.K. Hulet, J.F. Wild, K.J. Moody, R.J. Dougan, C.M. Gannett, R.A. Henderson, D.C. Hoffman, and D.M. Lee, *Fifty Years with Nuclear Fission* (American Nuclear Society, La Grange Park, IL, 1989) Vol.2, p.694.
- [12] Yu.A. Lazarev, Yu.V. Lobanov, A.N. Mezentsev, Yu.Ts. Oganessian, V.G. Subbotin, V.K. Utyonkov, F.Sh. Abdullin, V.V. Bekhterev, S. Iliev, I.V. Kolesov, A.N. Polyakov, I.M. Sedych, I.V. Shirokovsky, A.M. Sukhov, Yu.S. Tsyganov, and V.E. Zhuchko, in *Proceedings of the International School-Seminar on Heavy Ion Physics*, Dubna, 1993 (JINR Report No. E7-93-274, Dubna, 1993) Vol.2, p.497.
- [13] N. Bohr, *Phys. Rev.* **59**, 270 (1941).
- [14] L.P. Somerville, M.J. Nurmia, J.M. Nitschke, A. Chiorso, E.K. Hulet, and R.W. Loughheed, *Phys. Rev. C* **31**, 1801 (1985).
- [15] M.R. Schmorak, *Nucl. Data Sheets* **57**, 515 (1989); **59**, 507 (1990).
- [16] E.K. Hulet, J.F. Wild, R.J. Dougan, R.W. Loughheed, J.H. Landrum, A. D. Dougan, P.A. Baisden, C.M. Henderson, R.J. Dupzyk, R.L. Hahn, M. Schädel, K. Stümmerer, and G.R. Bethune, *Phys. Rev. C* **40**, 770 (1989).
- [17] R. Smolańczuk and A. Sobiczewski, private communication, December 1995.
- [18] Yu.A. Lazarev, I.V. Shirokovsky, V.K. Utyonkov, S.P. Tretyakova, and V.B. Kutner, *Nucl. Phys.* **A568**, 501 (1995).
- [19] Yu.A. Lazarev, Yu.V. Lobanov, R.N. Sagaidak, V.K. Utyonkov, M. Hussonnois, Yu.P. Kharitonov, I.V. Shirokovsky, S.P. Tretyakova and Yu.Ts. Oganessian, *Phys. Scripta* **39**, 422 (1989).
- [20] S. Hofmann, private communication, October 1994.
- [21] A. Türler, these Proceedings.
- [22] E.D. Donets, V.A. Shchegolev, and V.A. Ermakov, *Yad. Fiz.* **2**, 1015 (1965) [*Sov. J. Nucl. Phys.* **2**, 723 (1965)].
- [23] T. Sikkeland, J. Maly, and D.F. Lebeck, *Phys. Rev.* **169**, 1000 (1968).
- [24] R. Bass, *Lecture Notes in Physics* **117**, 281 (1980).
- [25] S. Ōwrik; S. Hofmann, and W. Nazarewicz, *Nucl. Phys.* **A573**, 356 (1994).
- [26] S. Hofmann, V. Ninov, F.P. Hessberger, P. Armbruster, H. Folger, G. Münzenberg, H.J. Schött, A.G. Popeko, A.V. Yeremin, A.N. Andreyev, S. Saro, R. Janik, and M. Leino, *Z. Phys.* **A350**, 277 (1995); *GSJ Nachrichten 02-95* (Darmstadt 1995) p.4.

- [27] A. Ghiorso, D. Lee, L.P. Somerville, W. Loveland, J.M. Nitschke, W. Ghiorso, G.T. Seaborg, P. Wilmarth, R. Leres, A. Wydler, M. Nurmia, K. Gregorich, K. Czerwinski, R. Gaylord, T. Hamilton, N.J. Hannink, D.C. Hoffman, C. Jarzynsky, C. Kacber, B. Kadkhodayan, S. Kreek, M. Lane, A. Lyon, M.A. McMahan, M. Neu, T. Sikkeland, W.J. Swiatecki, A. Türler, J.T. Walton, and S. Yashita, *Phys. Rev. C* **51**, R2293 (1995).

**Лазарев Ю.А.**

Пределы ядерной структуры:  
обнаружение замкнутых оболочек  $N = 162$  и  $Z = 108$

E7-96-82

Совместные эксперименты Дубна—Ливермор, выполненные в 1993—95 гг. с использованием дубненского газоуплотненного сепаратора продуктов ядерных реакций, привели к открытию новых нуклидов  $^{262}104$ ,  $^{266}106$ ,  $^{267}108$  и  $^{273}110$ . Это наиболее тяжелые изотопы элементов 104, 106, 108 и 110, известные в настоящее время. Идентификация  $^{273}110$  означает наблюдение элемента 110. Радиоактивные свойства синтезированных нами новых нуклидов дают доказательства существования замкнутых оболочек  $N = 162$  и  $Z = 108$ , предсказанных современной макро-микроскопической теорией ядра. Результаты данной серии экспериментов открывают новые возможности расширения области наиболее тяжелых ядер и делают продвижение к предсказанным сферическим оболочкам  $N \approx 178-184$  и  $Z \approx 114$  актуальным направлением будущих экспериментальных исследований.

Работа выполнена в Лаборатории ядерных реакций им. Г.Н.Флерова ОИЯИ.

Препринт Общественного института ядерных исследований. Дубна, 1996

**Лазарев Ю.А.**

Extremes of Nuclear Structure:  
Discovery of the Shell Closures  $N = 162$  and  $Z = 108$

E7-96-82

Collaborative Dubna—Livermore experiments performed in 1993—1995 by employing the Dubna gas-filled recoil separator have resulted in the discovery of the new nuclides  $^{262}104$ ,  $^{266}106$ ,  $^{267}108$  and  $^{273}110$ . These nuclides represent the heaviest isotopes of elements 104, 106, 108 and 110 produced up to now. The identification of  $^{273}110$  signifies the observation of the shell closures at  $N = 162$  and  $Z = 108$  predicted by modern macroscopic-microscopic nuclear theory. The findings of the present series of experiments create novel opportunities for extending the nuclear domain at its upper edge and offer the predicted spherical shells at  $N \approx 178-184$  and  $Z \approx 114$  to be a major challenge for future experimental explorations.

The investigation has been performed at the Flerov Laboratory of Nuclear Reactions, JINR.

Preprint of the Joint Institute for Nuclear Research. Dubna, 1996

Received by Publishing Department  
on March 6, 1996